

An experimental method to determine the effective luminescence efficiency of scintillator–photodetector combinations used in X-ray medical imaging systems

¹D CAVOURAS, PhD, ¹I KANDARAKIS, PhD, ²A BAKAS, MSc, ³D TRIANTIS, PhD, ³C D NOMICOS, PhD and ⁴G S PANAYIOTAKIS, PhD

Departments of ¹Medical Instrumentation Technology, ²Radiology and ³Electronics, Technological Educational Institution of Athens, Agiou Spyridonos Street, Aigaleo 122 10, Athens, and ⁴Department of Medical Physics, Medical School, University of Patras, 265 00 Patras, Greece

Abstract. The scintillator effective luminescence efficiency, which may be defined in terms of the scintillator's X-ray luminescence efficiency and the scintillator–photodetector spectral matching and geometrical configuration, was studied for various X-ray imaging applications. Four scintillator materials Gd₂O₂S:Tb, Y₂O₂S:Tb, ZnSCdS:Ag and CsI:Na were used to prepare test screens. They were evaluated in relation to various photodetectors used in X-ray imaging, such as radiographic films, photocathodes, and photodiodes. Effective luminescence efficiency was determined for a range of X-ray tube voltages (50–140 kVp) by measuring the light flux emitted per unit of incident exposure rate and the spectra of the light emitted by the four scintillators. Scintillator–photodetector combinations resulting in higher image brightness level were determined for different X-ray imaging systems. Findings indicate that CsI:Na is very efficient with orthochromatic radiographic films, Gd₂O₂S:Tb could be useful in conventional or digital fluoroscopy and in CT and ZnSCdS:Ag could be employed in some medium to low voltage digital radiography applications.

Most X-ray imaging systems use scintillators, often in the form of fluorescent screens, in combination with photodetectors. Examples of such combinations are intensifying screens combined with films in radiographic cassettes [1, 2]; input phosphor screens coupled to photocathodes in image intensifiers for conventional fluoroscopy, digital radiography, and digital fluoroscopy; phosphor screens connected to charge coupled device (CCD) arrays in digital radiography [3]; scintillator–photodiode combinations in CT solid state detectors [4]. Image brightness depends strongly on the light producing ability of the scintillator material, on its spectral compatibility with the photodetector as well as on the geometry of the scintillator–photodetector system. Light producing ability may be assessed by the absolute X-ray luminescence efficiency, defined as the light energy flux emitted by a scintillator towards the photodetector per unit of incident X-ray energy flux or exposure rate [5–7]. The latter is related to the patient dose burden during X-ray examinations. Spectral compatibility expresses the ability of the photodetector to capture the specific light wavelengths emitted by the scintillator. It depends on the spectral sensitivity distribution of the photodetector [8]. An experimental method to predict in

an accurate and systematic manner the most efficient scintillator–photodetector combination at various X-ray energies and for different X-ray imaging systems needs to be determined.

In the present study, the effective X-ray luminescence efficiency was defined to take into account the light producing ability of the scintillator, the spectral compatibility effects between the scintillator and the photodetector, and the light losses due to the geometry of the scintillator–photodetector system. Effective luminescence efficiency was studied at various X-ray tube voltages and for various scintillator–photodetector combinations that are used or could be used in medical X-ray imaging. Combinations giving highest output light flux corresponding to minimum radiation dose burden to the patient were determined for various X-ray imaging applications.

Material and methods

Theory: the effective luminescence efficiency

The light energy flux (Ψ_L) emitted by an irradiated fluorescent screen depends on the following:

- (1) the incident X-ray energy flux (Ψ_x);
- (2) the X-ray quantum detection efficiency (QDE), which is the ratio (η_Q) of the detected to the incident X-ray photons;

Received 28 August 1997 and in final form 6 March 1998, accepted 13 March 1998.

- (3) the intrinsic X-ray to light conversion efficiency (η_C) giving the fraction of absorbed X-ray energy flux converted into light within the scintillator material;
- (4) the light transmission efficiency (G_L) expressing the fraction of light produced within the screen that is transmitted to the screen emitting surface.

Hence, the emitted light flux may be expressed as:

$$\Psi_L = \Psi_X(E)\eta_Q(E, t)\eta_C G_L(a, s, E, t) \quad (1)$$

where, E is the energy of the incident X-ray photons, t is the thickness of the fluorescent screen, a and s are the light absorption and light scattering coefficients depending on the scintillator material, the screen structure (granular or non-granular), and the wavelength of the emitted light. However, only a fraction of Ψ_L may be captured and utilized by the photodetector due to: (1) the spectral compatibility imperfections between the emitted light wavelengths and the photodetector's spectral sensitivity, and (2) the geometrical arrangement of the scintillator-photodetector combination. This fraction of Ψ_L is defined as the effective light energy flux Ψ_{Leff} , which is the diagnostically useful signal given by:

$$\Psi_{Leff} = c_{SP} c_{GL} \Psi_L \quad (2)$$

where, c_{SP} is the spectral compatibility coefficient, describing the efficiency with which the photodetector can capture the spectral wavelengths emitted by the screen. c_{GL} is the geometric light collection efficiency (GCE), describing light losses due to system geometry such as the distance between the screen and the photodetector, the area of the screen covered by the photodetector, intervening fibre optics or optical lenses etc. [3].

In defining c_{SP} , the spectral sensitivity ($S_D(\lambda)$), giving the variation of the photodetector's sensitivity as function of light wavelength (λ) has to be considered. If $S_D(\lambda)$ is divided by the total detector sensitivity S_O , obtained by summing up all $S_D(\lambda)$ contributions from all light wavelengths corresponding to non-zero $S_D(\lambda)$ values, then the relative spectral sensitivity $S_R(\lambda)$ of the detector at wavelength λ may be defined as:

$$S_R(\lambda) = \frac{S_D(\lambda)}{\int_{\lambda} S_D(\lambda) d\lambda} \quad (3)$$

If $S_P(\lambda)$ is the function describing the shape of the light spectrum emitted by the scintillator normalized to unity, then the product $S_P(\lambda)S_R(\lambda)$ gives the relative contribution of the light of wavelength λ to the total optical signal captured by the photodetector. The spectral compatibility coefficient c_{SP}

may then be defined as the total relative signal captured, obtained by summing up the relative contributions from all emitted light wavelengths λ :

$$c_{SP} = \int_{\lambda} S_P(\lambda)S_R(\lambda) d\lambda \quad (4a)$$

Thus, from relations (1), (2) and (4a) the total optical signal captured by the photodetector, represented by the effective light energy flux Ψ_{Leff} in (2), is given by:

$$\Psi_{Leff} = \Psi_X(E)\eta_Q(E, t)\eta_C G_L(a, s, E, t) \times \left[\int_{\lambda} S_P(\lambda)S_R(\lambda) d\lambda \right] c_{GL} \quad (4b)$$

Then the effective luminescence efficiency $\eta_{\Phi eff}$ can be defined as the ratio of the total optical signal captured (Ψ_{Leff}) over the incident X-ray energy flux (Ψ_X):

$$\eta_{\Phi eff} = \frac{\Psi_{Leff}}{\Psi_X} = \eta_{\Phi} c_{SP} c_{GL} \quad (5)$$

where η_{Φ} is the absolute X-ray luminescence efficiency of a fluorescent screen given by:

$$\eta_{\Phi} = \frac{\Psi_L}{\Psi_X} = \eta_Q(E, t)\eta_C G_L(a, s, E, t) \quad (6)$$

To represent experimental conditions, where the exposure rate rather than the X-ray energy flux is measured, the effective luminescence efficiency in (5) and (6) must be defined in a way that the quantity Ψ_X is converted into exposure rate using the appropriate conversion factor [9]:

$$\alpha = \frac{\dot{X}}{\Psi_X} = \left[\frac{\mu_{en}}{\rho} \right]_{air} \frac{e}{W_{air}} \quad (7)$$

where, $[\mu_{en}/\rho]_{air}$ is the mass energy absorption coefficient of air, e is the electron charge and W_{air} is the average energy required to produce an ion pair in air.

Finally, since polyenergetic X-ray beams are used in diagnostic radiology, the effective luminescence efficiency must be averaged over the X-ray energy spectrum [3, 6, 7, 10].

For a number of X-ray imaging systems the geometric light collection efficiency c_{GL} in relations (2), (4b) and (5) is close to unity since the photodetector is either in very good contact with the scintillator as in radiographic screen-film systems or it is directly deposited on the scintillator as in image intensifiers [3], phosphor coated CCDs [11]. However, in digital radiography detectors that employ optical lenses or fibre optics between the screen and the CCD array [3] as well as in CT detectors [4], c_{GL} is significantly reduced [3, 12, 13]. This affects the corresponding effective luminescence efficiency. For an optical lens c_{GL}

may be expressed [3, 12] as:

$$c_{GL} = \frac{\tau}{4f^2(m+1)^2} \quad (8)$$

where, τ is the optical transmission factor of the lens, f is the ratio of the lens focal length to the aperture diameter ("f-number"), and m is a factor accounting for the image demagnification from the scintillator to the photodetector. Values of the order of 0.1% have been reported [3, 12] for c_{GL} . For a fibre optic taper c_{GL} has been expressed as

$$c_{GL} = \frac{A_{OP}\tau n^2}{m^2} \quad (9)$$

where, A_{OP} is the fraction of the taper input surface corresponding to the core glass of the fibre optics, n is the numerical aperture of the untapered fibre, and τ and m are defined in relation (8). c_{GL} has been determined [3] to be of the order of 0.7%. For CT detectors, c_{GL} depends on the refractive index of the transparent layer intervening between the scintillator and the photodiode as well as on the detector element width. c_{GL} values ranging between 0.42 and 0.80 have been reported [14]. Although the value of c_{GL} may slightly depend on the emitted light wavelength, for the scintillators employed in this work c_{GL} was considered approximately constant. The reason for this is that c_{GL} depends either on purely geometrical or optical transmission factors. Both factors were considered to remain practically constant for the wavelengths included in the spectra of the scintillators employed in this study.

Deciding on best scintillator–photodetector combination, considerations should be made concerning image quality, such as spatial resolution and quantum noise. Spatial resolution is degraded with screen thickness, since in thick screens light spread due to isotropic light propagation and optical scattering effects is augmented. However, in some non-granular screens, such as CsI:Na, scattering is minimized and light propagation is highly directional due to screen internal structure causing a reduction in light spread.

The impact of quantum noise may be assessed by the signal-to-noise ratio (SNR). SNR increases with quantum detection efficiency (η_Q) of the scintillating screen but it is also related to the number of light photons emitted per X-ray at screen output [3]; the number of light photons is associated with the X-ray to light conversion efficiency (η_C), the light transmission efficiency (G_L), and hence the X-ray luminescence efficiency (η_Φ).

Experimental method

The scintillator materials employed for preparing fluorescent screens were Gd₂O₂S:Tb, Y₂O₂S:Tb, ZnSCdS:Ag and CsI:Na. These

materials have been commercially used in the phosphor screens of radiographic cassettes, in the input screens of image intensifiers, and in the detectors of digital imaging systems.

Scintillators were supplied in powder form (Derby Luminescents Ltd, Derby, UK) with grains of around 7 μm in diameter. Fluorescent screens with coating weights of approximately 75 mg cm⁻² and 110 mg cm⁻² were prepared in our laboratory. Gd₂O₂S:Tb, Y₂O₂S:Tb, ZnSCdS:Ag screens were produced by sedimentation on fused silica substrates employing a mixture of 2 l of de-ionized water, 25 ml Na₂SiO₃ aqueous solution (binding material between the powder grains), and the appropriate amount of powder for the desired screen coating weight. CsI:Na screens were formed by evaporation, employing a quantity of pure CsI and NaI for the activator (Na). Screens prepared by sedimentation were of granular form with packing density of about 50% in scintillator grains and 50% in binding material. Screens prepared by evaporation consisted of pure scintillator material with over 90% packing density.

The effective luminescence efficiency was determined in accordance with relation (5). At first, the absolute luminescence efficiency was found by measuring the light flux, emitted by the irradiated screens, and the incident exposure rate. Screens were X-rayed by a Siemens Stabilipan machine with tube voltages ranging from 50 kVp to 140 kVp. A 20 mm Al filter was employed to simulate X-ray attenuation by human tissue [6]. The light flux (Ψ_L) and the exposure rate (\dot{X}) were measured by an EMI 9558 QB photomultiplier, coupled to a Cary 401 electrometer, and by a PTW dosimeter (ionization chamber type No. 23333), respectively. Light flux was measured on the side opposite to the irradiated screen surface [6]. Next, the spectral compatibility coefficient (c_{sp}) was determined according to relations (3) and (4); the spectrum of the emitted light ($S_p(\lambda)$) was measured by an Oriel 7240 Grating monochromator, and the spectral sensitivities ($S_p(\lambda)$) of the photodetectors were obtained from manufacturers' data.

Results and discussion

Figure 1 shows the absolute X-ray luminescence efficiency variation with X-ray tube voltage for Gd₂O₂S:Tb, Y₂O₂S:Tb, ZnSCdS:Ag, CsI:Na screens of 75 mg cm⁻² coating weight. Highest efficiency values were obtained for the Gd₂O₂S:Tb screen (51 EU, where 1 EU = 3.875 J/C kg⁻¹ m² in SI units) in the range 120–140 kVp. This result is very interesting for CT, since relatively high voltages are used. However, for the range below 100 kVp, which is very useful for many radiographic and fluoroscopic techniques, the CsI:Na screen was clearly better than the Gd₂O₂S:Tb,

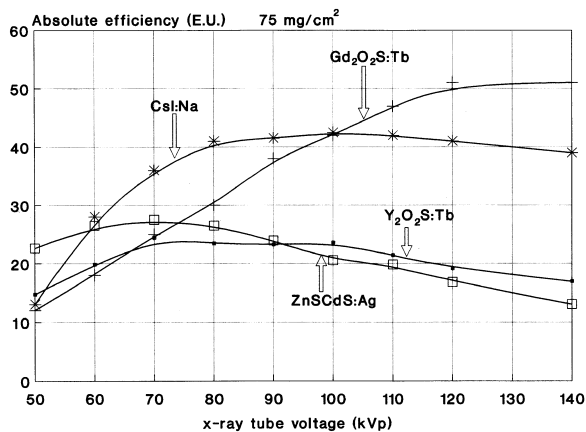


Figure 1. Absolute X-ray luminescence efficiency variation with X-ray tube voltage for $\text{Gd}_2\text{O}_2\text{S:Tb}$, $\text{Y}_2\text{O}_2\text{S:Tb}$, ZnSCdS:Ag , CsI:Na screens with approximately 75 mg cm^{-2} coating weight. (EU, efficiency unit, $1 \text{ EU} = 1 \mu\text{W m}^{-2}/\text{mR s}^{-1}$ or $3.875 \text{ J/C kg}^{-1} \text{ m}^2$ SI units.) Points represent experimental data.

attaining its highest values (41–43 EU) in the range 80–100 kVp. It is interesting to notice that the ZnSCdS:Ag screen was found to be more efficient than the $\text{Gd}_2\text{O}_2\text{S:Tb}$ and CsI:Na screens for tube voltages lower than 75 kVp and 60 kVp, respectively. It must be also noted that the temporal responses of the scintillators considered here (0.4 ms for $\text{Gd}_2\text{O}_2\text{S:Tb}$ and ZnSCdS:Ag , 0.5 ms for $\text{Y}_2\text{O}_2\text{S:Tb}$, and 0.6 μs for CsI:Na [1]) are adequate for both fluoroscopy and CT applications. Finally, the $\text{Y}_2\text{O}_2\text{S:Tb}$ screen was found to be better than the $\text{Gd}_2\text{O}_2\text{S:Tb}$ and CsI:Na screens for the ranges below 67 and 53 kVp, respectively, and better than ZnSCdS:Ag for voltages higher than 90 kVp. ZnSCdS:Ag and $\text{Y}_2\text{O}_2\text{S:Tb}$ highest values were 36 EU and 33 EU, respectively, both obtained at 70 kVp. Regarding the 110 mg cm^{-2} screens shown in Figure 2, CsI:Na was found superior to $\text{Gd}_2\text{O}_2\text{S:Tb}$ for tube voltages between 54 and

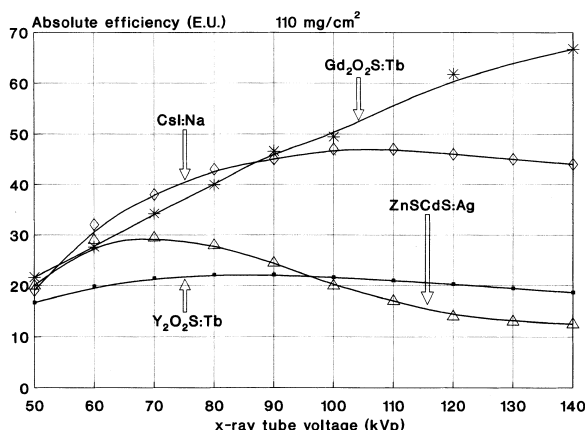


Figure 2. Absolute X-ray luminescence efficiency variation with X-ray tube voltage for $\text{Gd}_2\text{O}_2\text{S:Tb}$, $\text{Y}_2\text{O}_2\text{S:Tb}$, ZnSCdS:Ag , CsI:Na screens with approximately 110 mg cm^{-2} coating weight. (EU, efficiency unit, $1 \text{ EU} = 1 \mu\text{W m}^{-2}/\text{mR s}^{-1}$ or $3.875 \text{ J/C kg}^{-1} \text{ m}^2$ SI units.) Points represent experimental data.

87 kVp. Comparing Figures 1 and 2 it can be observed that the 110 mg cm^{-2} $\text{Gd}_2\text{O}_2\text{S:Tb}$ scintillator is superior to the other materials within a wider range of X-ray tube voltages. It is also worth noting that the 110 mg cm^{-2} $\text{Gd}_2\text{O}_2\text{S:Tb}$ screen seems to give very good results in the low voltage region as well; at 50 kVp the efficiency of $\text{Gd}_2\text{O}_2\text{S:Tb}$ was measured to be higher than the corresponding efficiencies of CsI:Na and ZnSCdS:Ag .

Differences in absolute efficiency among the four scintillators may be explained by considering the following parameters: (1) the atomic numbers (Z) and densities (ρ) of the materials that determine the X-ray absorption coefficients, which in turn determine the quantum detection efficiency, η_Q in relations (1) and (6). $\text{Gd}_2\text{O}_2\text{S:Tb}$ screens having high Z and ρ values exhibit the highest absorption coefficients in a wide range of X-ray energies followed by CsI:Na and ZnSCdS:Ag screens. These absorption coefficients have been calculated from published data [15]. (2) The intrinsic X-ray to light conversion efficiency (η_C), which is very high for $\text{Gd}_2\text{O}_2\text{S:Tb}$, ZnSCdS:Ag , and $\text{Y}_2\text{O}_2\text{S:Tb}$, of the order of 0.15–0.20 [1, 2, 6, 7], but attains medium values for CsI:Na ($\eta_C = 0.10$) [1, 2]. (3) The optical scattering effects that affect the light transmission efficiency (G_L) in relations (1) and (6). Scattering effects must be more pronounced in $\text{Gd}_2\text{O}_2\text{S:Tb}$, $\text{Y}_2\text{O}_2\text{S:Tb}$ and ZnSCdS:Ag , since in these screens the scintillator is in the form of grains that increase the amount of optical scattering. On the other hand, CsI:Na screens are of almost compact form, which minimizes scattering and, thus, decreases optical photon losses during light transmission. The decreased scattering in CsI:Na ameliorates luminescence efficiency values, compared with ZnSCdS:Ag and $\text{Y}_2\text{O}_2\text{S:Tb}$, despite the fact that the intrinsic conversion efficiency of ZnSCdS:Ag and $\text{Y}_2\text{O}_2\text{S:Tb}$ is double that of CsI:Na .

Figure 3 shows the measured spectra of the light emitted by the $\text{Gd}_2\text{O}_2\text{S:Tb}$, CsI:Na , ZnSCdS:Ag , and $\text{Y}_2\text{O}_2\text{S:Tb}$ screens together with spectral sensitivity curves of some of the photodetectors employed. The detectors studied were the S9, S11, and the extended sensitivity E/S20 photocathodes, used in image intensifiers or in photomultipliers (e.g. in gamma cameras), the Si photodiode, used in CCD arrays of digital radiography systems and in solid state CT detectors, the Agfa Curix Ortho GS, Kodak X-omatic GR and Fuji UM-NH orthochromatic radiographic films. Although three films were used to determine the spectral compatibility coefficient only one is shown, because the corresponding curves were very similar. Similar reasoning applies to photocathodes used in this work. Spectral sensitivity curves were obtained from manufacturers' data (EMI, RCA, Hamamatsu, ITL, Rofin, Kodak, Fuji, Agfa).

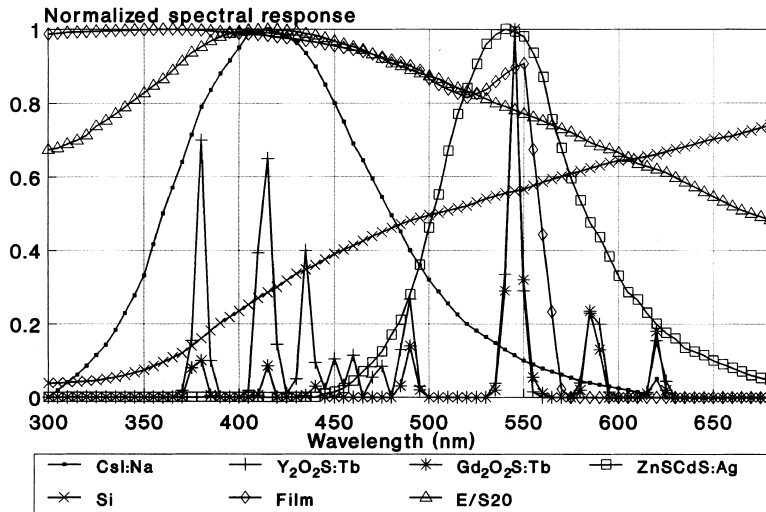


Figure 3. Scintillator measured emission spectra and photodetector spectral sensitivities normalized to unity.

Figure 4 compares the effective efficiencies of the 75 mg cm⁻² fluorescent screens combined with the E/S20 photocathode. In the range 55–115 kVp, the dominant combination is the CsI:Na-E/S20 giving maximum values (38–40 EU) between 80 and 110 kVp. Thus, fluoroscopic image intensifiers equipped with the E/S20 photocathode coupled to a CsI:Na screen should form imaging devices with the lowest dose burden to the patient for a desired image brightness level. Additionally, by employing CsI:Na screens, both spatial resolution and SNR should improve due to (1) the absence of high scattering powder grains and the presence of tiny needle like columns formed in the intrinsic structure of CsI:Na that restrict lateral spread and improve resolution, and (2) the relatively high effective atomic number that increases QDE and hence SNR. However, for voltages lower than 55 kVp, the ZnSCdS:Ag-E/S20 combination seems to give better results. Nevertheless, spatial resolution employing ZnSCdS:Ag screens should be

lower compared with CsI:Na due to the presence of scattering grains in ZnSCdS:Ag. Results on S9 and S11 photocathodes are not shown being slightly inferior to E/S20.

In the case of the Si photodiode (Figure 5) the most efficient combination is with the Gd₂O₂S:Tb screen for voltages higher than 77 kVp while at lower energies the ZnSCdS:Ag-Si combination proved superior. Hence, these two scintillators (Gd₂O₂S:Tb and ZnSCdS:Ag) could be used in digital imaging systems employing Si photodetectors. ZnSCdS:Ag could be suitable for digital radiography employing medium to low tube potential settings while Gd₂O₂S:Tb could be appropriate for CT detectors as well as for digital radiography employing X-rays with tube potential settings higher than 75 kVp. However, systems with Gd₂O₂S:Tb will be of higher resolution than systems with ZnSCdS:Ag in the whole tube potential range. This is due to the high density of Gd₂O₂S:Tb resulting in thinner screens for equal coating weight. Additionally, SNR of Gd₂O₂S:Tb will be

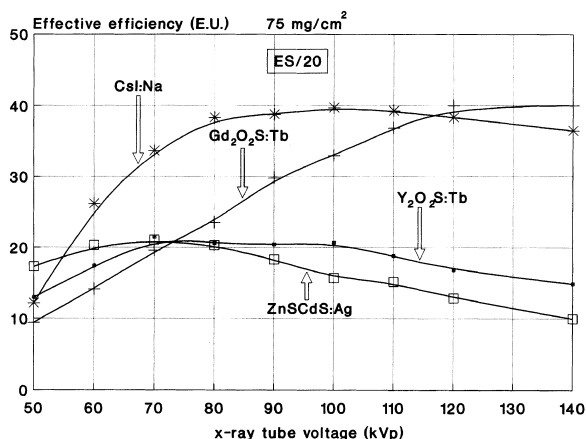


Figure 4. Effective luminescence efficiencies of the 75 mg cm⁻² Gd₂O₂S:Tb, Y₂O₂S:Tb, ZnSCdS:Ag, CsI:Na screens combined with the extended sensitivity E/S20 photocathode. (EU, efficiency unit, 1 EU = 1 μW m⁻²/mR s⁻¹ or 3.875 J/C kg⁻¹ m² SI units.) Points represent experimental data.

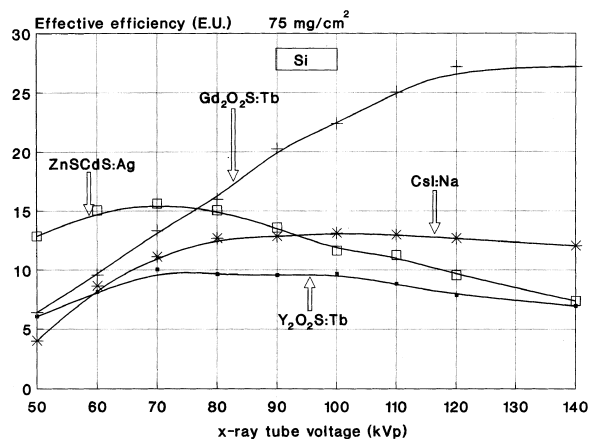


Figure 5. Effective luminescence efficiencies of the 75 mg cm⁻² Gd₂O₂S:Tb, Y₂O₂S:Tb, ZnSCdS:Ag, CsI:Na screens combined with the Si photodiode. (EU, efficiency unit, 1 EU = 1 μW m⁻²/mR s⁻¹ or 3.875 J/C kg⁻¹ m² SI units.) Points represent experimental data.

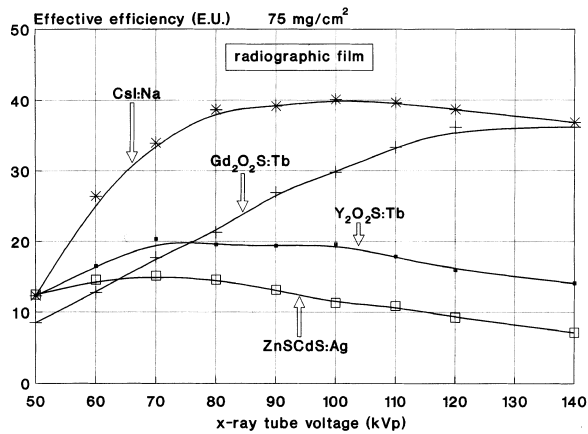


Figure 6. Effective luminescence efficiencies of the 75 mg cm^{-2} $\text{Gd}_2\text{O}_2\text{S:Tb}$, $\text{Y}_2\text{O}_2\text{S:Tb}$, ZnSCdS:Ag , CsI:Na screens combined with the green sensitive orthochromatic film. (EU, efficiency unit, $1 \text{ EU} = 1 \mu\text{W m}^{-2}/\text{mR s}^{-1}$ or $3.875 \text{ J/C kg}^{-1} \text{ m}^2$ SI units.) Points represent experimental data.

better due to its higher effective atomic number resulting in higher quantum detection efficiency. Results in Figure 5 were obtained by considering $\text{GCE} = 1.0$. For digital imaging systems incorporating fibre optics, lenses, transparent layers etc., c_{GL} in relation (5) is considerably reduced, thus affecting in a similar way the values of effective efficiency for all scintillators.

The CsI:Na screen coupled to one orthochromatic film (Figure 6) is the most efficient 75 mg cm^{-2} screen-film combination in the entire voltage range from 50 kVp up to 140 kVp, attaining maximum values (38–40 EU) in the 80–120 kVp range. Considering also the high resolution exhibited by CsI:Na screens, this combination could be an excellent image receptor for conventional radiography cassettes, provided the problems imposed by the hygroscopic properties of CsI:Na are properly solved by using light transparent protective covers.

Results found but not shown on the effective efficiencies of the 110 mg cm^{-2} screens revealed that the $\text{Gd}_2\text{O}_2\text{S:Tb}$ screen had better effective efficiencies than the other scintillators in a wider range of tube voltages as compared to data obtained for the 75 mg cm^{-2} screens. Also, it was found that the effective efficiency increases with coating weight, mainly due to the higher detection efficiency, η_{Q} of thicker screens. However, the light transmission efficiency G_{L} causes an inverse effect, because it is more difficult for light photons produced within the scintillator to penetrate thicker screens. Thus, the increase in effective efficiency with screen coating weight sometimes may be minimized.

In conclusion, CsI:Na screens could provide a very good combination with the orthochromatic radiographic films, which are regularly used with the terbium activated scintillators $\text{Gd}_2\text{O}_2\text{S:Tb}$ and $\text{Y}_2\text{O}_2\text{S:Tb}$, provided that hygroscopy problems are

solved. $\text{Gd}_2\text{O}_2\text{S:Tb}$ could also be used not only in conventional or digital radiographic receptors but in conventional or digital fluoroscopy as well, especially at rather high tube voltages and high screen coating weights. Additionally, $\text{Gd}_2\text{O}_2\text{S:Tb}$ may be appropriate for use in CT solid state detectors. The ZnSCdS:Ag scintillator could be proved useful in some digital radiography applications, especially at rather low tube voltages and screen coating weights.

Acknowledgment

This study is dedicated to the memory of Professor G E Giakoumakis, leading member of our team, whose work on phosphor materials has inspired us all to continue.

References

1. Arnold BA. Physical characteristics of screen-film combinations. In: Haus AG, editor. The physics of medical imaging: recording system, measurements and techniques. New York: American Association of Physicists in Medicine, 1979:30–71.
2. Zweig G, Zweig DA. Radioluminescent imaging: factors affecting total light output. Proc SPIE 1983;419:297–304.
3. Yaffe MJ, Rowlands JA. X-ray detectors for digital radiography. Phys Med Biol 1997;42:1–39.
4. Haque P, Stanley JH. Scintillation crystal-photodiode array detectors. In: Newton TH, Potts DG, editors. Radiology of the skull and brain: technical aspects of computed tomography. St Louis: CV Mosby Company, 1981:4127–32.
5. Ludwig GW. X-ray efficiency of powder phosphors. J Electrochem Soc 1971;118:1152–9.
6. Kandarakis I, Cavouras D, Panayiotakis G, Agelis T, Nomicos C, Giakoumakis G. X-ray induced luminescence and spatial resolution of $\text{La}_2\text{O}_2\text{S:Tb}$ phosphor screens. Phys Med Biol 1996;41:297–307.
7. Cavouras D, Kandarakis I, Panayiotakis G, Evangelou EK, Nomicos CD. An evaluation of the $\text{Y}_2\text{O}_3:\text{Eu}^{3+}$ scintillator for application in medical X-ray detectors and image receptors. Med Phys 1996;23:1965–75.
8. Giakoumakis GE. Matching factors for various light-source-photodetector combinations. Appl Phys 1991;A52:7–9.
9. Hendee WR. Medical radiation physics. Chicago: Year Book Medical Publishers, 1970:145–8.
10. Kandarakis I, Cavouras D, Panayiotakis GS, Nomicos C. Evaluating X-ray detectors for radiographic applications: a comparison of ZnSCdS:Ag with $\text{Gd}_2\text{O}_2\text{S:Tb}$ and $\text{Y}_2\text{O}_2\text{S:Tb}$ screens. Phys Med Biol 1997;42:1351–73.
11. Gambaccini M, Taibi A, Del Guerra A, Marziani M, Tuffanelli. MTF evaluation of a phosphor-coated CCD for X-ray imaging. Phys Med Biol 1996;41:2799–806.
12. Karellas A, Harris LJ, Liu H, Davis MA, D'Orsi CJ. Charge-coupled device detector: Performance considerations and potential for small-field mammographic imaging applications. Med Phys 1992; 19:1015–23.

13. Gurwich AM. Luminescent screens for mammography. *Radiat Meas* 1995;24:325–30.
14. Takahashi T, Itoh H, Shimada T, Takeuchi H. Design of integrated radiation detectors with a Si-photodiodes on ceramic scintillators for use in X-ray computed tomography. *IEEE Trans Nucl Sci* 1990;NS-37:1478–82.
15. Storm E, Israel H. Photon cross-sections from 0.001 to 100 MeV for elements 1 through 100. Report LA-3753. Los Alamos, CA, USA: Los Alamos Scientific Laboratory of the University of California, 1967.